

# Dynamic mechanical study of amorphous phases in poly(ethylene terephthalate)/nylon-6 blends

T. Serhatkulu, B. Erman, I. Bahar\* and S. Fakirov†

*Polymer Research Center, School of Engineering, Bogazici University, and TUBITAK Advanced Polymeric Materials Research Center, Bebek 80815, Istanbul, Turkey*

and M. Evstatiev and D. Sapundjieva

*Sofia University, Laboratory on Structure and Properties of Polymers, 1126 Sofia, Bulgaria  
(Received 11 May 1994; revised 10 October 1994)*

The changes in the thermomechanical behaviour of a poly(ethylene terephthalate)/nylon-6 (PET/PA) blend (1:1 by weight) subjected to mechanical and thermal treatments are examined by means of dynamic mechanical measurements. It is established from previous studies that PET/PA blends are incompatible in the isotropic state, but form so-called microfibrillar-reinforced composites upon extrusion, drawing and suitable annealing. This study focuses mainly on the amorphous component of these blends and thus complements that recently performed (*Polymer* 1993, **34**, 4669) in which the crystalline phases were analysed. The orientation and crystallization of the homopolymers induced by drawing improve the dispersion of components and induce some compatibility as far as one glass transition temperature is observed. Yet, by annealing the drawn blend at temperatures below the melting temperatures of both components (220°C, for instance) the biphasic character of the composite is enhanced in as much as the microstructures of both the crystalline and amorphous phases are improved and the reorganization of species within separate phases is favoured. The components of the heterogeneous blend become compatible provided that the annealing is performed at a sufficiently high temperature (240°C). This temperature is intermediate between the melting temperature of the two components and allows for the isotropization of the low-melting component PA. The increase of compatibility is attributed to transreactions producing compatibilizing layers of PET/PA copolymers at phase boundaries between microfibrils and the amorphous matrix. Prolonged annealing (25 h) leads to the randomization of the original block copolymers and results in the complete participation of PA in the copolymer, which is evidenced by the disappearance of the glass transition peak of PA.

(Keywords: PET nylon-6 blend; dynamic mechanical analysis; solid-state reactions)

## INTRODUCTION

A new type of polymer composite called a microfibrillar-reinforced composite (MFC) was recently developed<sup>1-4</sup>. With respect to the size of the reinforcing elements, MFCs take an intermediate position between the two extreme groups of polymer composites: macrocomposites, e.g. glass fibre-reinforced composites, and molecular composites with liquid crystalline polymers as reinforcing elements. Bundles of highly oriented microfibrils act as reinforcing elements in MFCs.

Unlike the case of the classic composites, MFCs are formed from two immiscible, crystallizable homopolymers by drawing the polymer blend followed by annealing. Upon drawing, the components of the blend are oriented and microfibrils form<sup>1-4</sup>. The perfection of the structure is developed by subsequent annealing. The temperature

and duration of annealing have been shown significantly to affect the structure and properties of the blend: if the annealing temperature ( $T_a$ ) is set below the melting point ( $T_m$ ) of both components, the microfibrillar structure imparted by drawing is preserved and furthermore improved as a result of physical processes such as additional crystallization, minimization of defects in the crystalline regions and relaxation of residual stresses in the amorphous regions<sup>2</sup>. On the other hand, if  $T_a$  is set between the  $T_m$ s of the two components, isotropization of the low melting component takes place to form an isotropic matrix while the microfibrillar regions involving the component with higher  $T_m$  preserve their orientational and morphological characteristics<sup>2</sup>. The resulting material is referred to as a microfibrillar-reinforced composite.

Poly(ethylene terephthalate)/nylon-6 (PET/PA) blends, recently investigated<sup>2-4</sup> by differential scanning calorimetry (d.s.c.), small-angle and wide-angle X-ray scattering (SAXS and WAXS), infra-red spectroscopy and solubility measurements, represent a typical system illustrating the

\* To whom correspondence should be addressed

† Permanent address: Sofia University, Laboratory on Structure and Properties of Polymers, 1126 Sofia, Bulgaria

physical changes described above. Here PA is the component with lower melting point ( $T_m = 225^\circ\text{C}$ ), and PET that with higher melting temperature,  $T_m = 265^\circ\text{C}$ . Annealing of the drawn blend at  $T_a = 220^\circ\text{C}$  leads to a more pronounced increase in the crystallinity of both components whereas annealing at the intermediate temperature  $T_a = 240^\circ\text{C}$  between the  $T_m$  of the components is observed to yield a MFC comprising an isotropic matrix of PA reinforced with semicrystalline microfibrillized PET. The latter exhibits mechanical characteristics comparable to glass fibre-reinforced engineering plastics<sup>1,3</sup>. As may be inferred from the experimental techniques, these studies<sup>2,3</sup> provided information mainly about the changes in the crystalline phases of the components while the amorphous regions were almost non-characterized. The present study attempts to elucidate the changes in the amorphous phases in a PET/PA blend (1:1 by weight) subject to drawing and additional thermal treatment at various temperatures.

In addition to physical changes, the thermal treatment of blends of semicrystalline and/or amorphous condensation polymers might involve chemical changes which, in turn, affect the compatibility of components. In fact, exchange reactions between nearby functional groups, generating *in situ* copolymers, are reported to be a possible method for compatibilizing polyesters and polyamides<sup>5,6</sup>. As reviewed by Fakirov<sup>7</sup>, solid-state reactions in linear polycondensates are particularly favoured at high annealing temperatures and occur in the non-crystalline phases of the homopolymers, which enjoy relatively higher mobility, larger interface area and higher number of chain ends. Transesterification reactions have been observed in blends of bisphenol-A polycarbonate/poly(butylene terephthalate) (PBT)<sup>8-11</sup>, and PBT/polyarylate<sup>12,13</sup>. Evidence for solid-state exchange reactions and additional polycondensation was also observed in binary and ternary blends of PET, PBT and PA after the samples were annealed at  $240^\circ\text{C}$ <sup>14</sup>. In the main, a decrease in the degree of crystallinity and the enthalpy of melting of the thermally treated samples was observed by d.s.c., SAXS and WAXS, and was essentially caused by the diminishing contribution of the PA component. This weaker ability of the PA component to crystallize in thermally treated PET/PA blends was attributed<sup>3</sup> to its chemical interaction, in the molten state during the annealing process, with the amorphous fractions of PET to form PET-PA copolymers at the interfaces between the amorphous matrix and microfibrillar regions. Prolonged annealing, up to a duration of about 25 h, would have two effects: (i) the growth of the copolymer layers to eventually involve the whole matrix PA, and (ii) the transformation of the originally formed block copolymers into entropically favoured random copolymers which themselves are non-crystallizable upon cooling. In that case the PA component might be partly or fully trapped in these copolymers and this will strongly affect its backcrystallization, whereas for the PET component, of which a large fraction preserves its original microfibrillar structure, no significant change in crystallization properties would be observed. The gradual decrease in the crystallizability of PA with increasing annealing duration and its final disappearance as a crystallizable component conform with this description<sup>3</sup>. The formation of copolymer layers, improving the adhesion and compatibility between microfibrils and the

matrix, was also supported by the responses of the resulting MFC to external mechanical fields<sup>3</sup>. However, these interpretations, which were inferred from the behaviour of the crystalline phases only, would be more firmly established if confirmed by experiments directly investigating the behaviour of the amorphous regions. The present study aims to test the validity of the above chemical changes through examination of the amorphous phases that are directly involved in additional condensation and/or transreactions, if any.

## EXPERIMENTAL

The polymers used were PET (Goodyear Merge 1934F,  $\bar{M}_n = 23\,400$ ) and PA6 (AlliedSignal Capron 8200,  $\bar{M}_n = 20\,600$ ). After cooling in liquid nitrogen these polymers were finely ground and then mixed in the solid state (1:1 by weight). Films of this blend and of the respective neat homopolymers were prepared according to the following procedure: A capillary rheometer, flushed with argon and heated to about  $280^\circ\text{C}$ , was loaded with powdered material. The melt obtained was kept in the rheometer for 5–6 min and then extruded through the capillary (1 mm diameter) on metal rolls rotating at about  $300\text{ rev min}^{-1}$ . The rolls were immersed in a quenching bath of liquid nitrogen. In this way films of both neat homopolymers and of their blends were prepared, their thickness (0.10–0.13 mm) and width (4–5 mm) depending on the extrusion rate and distance between the rolls.

All films were oriented using the method of zone drawing<sup>14,15</sup> under the following conditions: zone drawing was performed on the quenched films by moving a narrow (diameter 2 mm) cylindrical heater attached to the crosshead of a Zwick tensile-testing machine, from the lower to the upper part of the samples under tension with a speed of  $10\text{ mm min}^{-1}$ . A tension of 15 MPa was applied to the films. The temperature of the heater was  $85^\circ\text{C}$  for PET and  $180^\circ\text{C}$  for both PA and the PET/PA blend. The zone-drawn films were subsequently annealed in vacuum with fixed ends at  $220$  or  $240^\circ\text{C}$  for a duration

**Table 1** Sample designation and preparation conditions

Sample designation	Zone drawing temperature ( $^\circ\text{C}$ )	Annealing in vacuum (with fixed ends)	
		$T_a$ ( $^\circ\text{C}$ )	$t_a$ (h)
PET			
PET (as quenched)	—	—	—
PET-I	85	—	—
PET-I-1	85	220	5
PET-I-2	85	220	25
PET-I-4	85	240	25
PA			
PA (as quenched)	—	—	—
PA-I	180	—	—
PA-I-1	180	220	5
PA-I-2	180	220	25
PET/PA blend			
B (as quenched)	—	—	—
B-I	180	—	—
B-I-1	180	220	5
B-I-2	180	220	25
B-I-3	180	240	5
B-I-4	180	240	25

of  $t_a = 5$  or 25 h. The sample preparation conditions and the corresponding nomenclature are given in Table 1.

The tensile storage modulus ( $E'$ ), loss modulus ( $E''$ ) and the tangent of the loss angle ( $\tan \delta$ ) of all samples were measured after ageing for 5 years at room temperature. The measurements were performed at 5 Hz and a heating rate of  $10^\circ\text{C min}^{-1}$ , using a Polymer Laboratories dynamic mechanical thermoanalyser (DMTA). Film lengths varied between 10 and 15 mm. The temperature range was from  $-50^\circ\text{C}$  to  $200^\circ\text{C}$ . The low-temperature measurements were performed in a stream of dry air cooled with liquid nitrogen, and the high-temperature measurements were carried out in a stream of dry nitrogen gas.

Photographic WAXS patterns were taken in transmission mode using a flat-film camera on a Kristallflex Siemens D500 diffractometer operating with Ni-filtered Cu K $\alpha$ -radiation.

## RESULTS

To improve understanding of the properties of the blend PET/PA, it was necessary first to follow the behaviour of the neat components subject to the same mechanical and thermal treatment. The temperature dependence of loss modulus  $E''$  for neat PET and neat PA samples subjected to various mechanical and thermal treatments is displayed in Figures 1a and b, respectively. In Figure

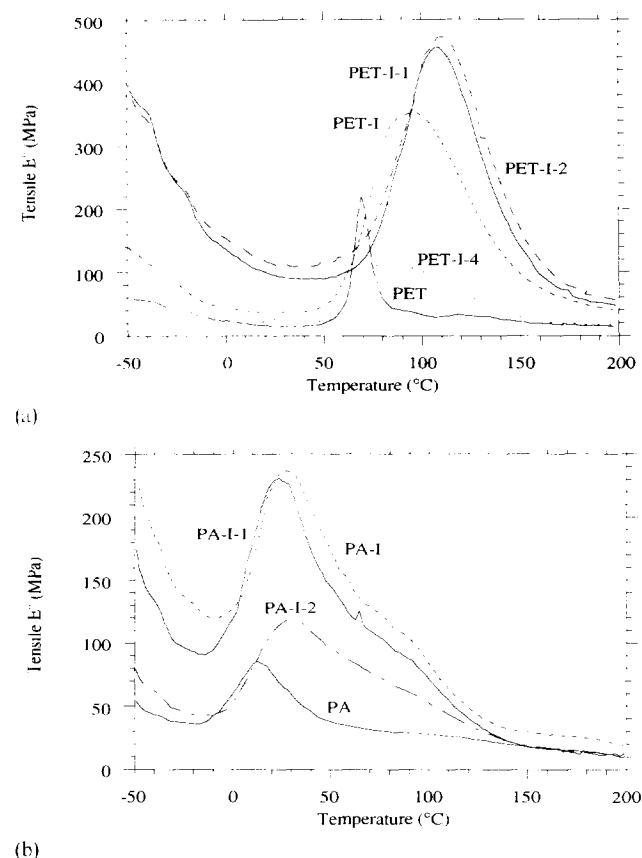


**Figure 1** Temperature dependence of the loss modulus  $E''$  of (a) neat PET and (b) neat PA subject to different thermal and mechanical treatments: PET, PA, undrawn, unannealed; PET-I, PA-I, zone drawn; PET-I-1, PA-I-1, drawn and annealed at  $T_a = 220^\circ\text{C}$ ,  $t_a = 5$  h; PET-I-2, PA-I-2, drawn and annealed at  $T_a = 220^\circ\text{C}$ ,  $t_a = 25$  h; PET-I-4, drawn and annealed at  $T_a = 240^\circ\text{C}$ ,  $t_a = 25$  h

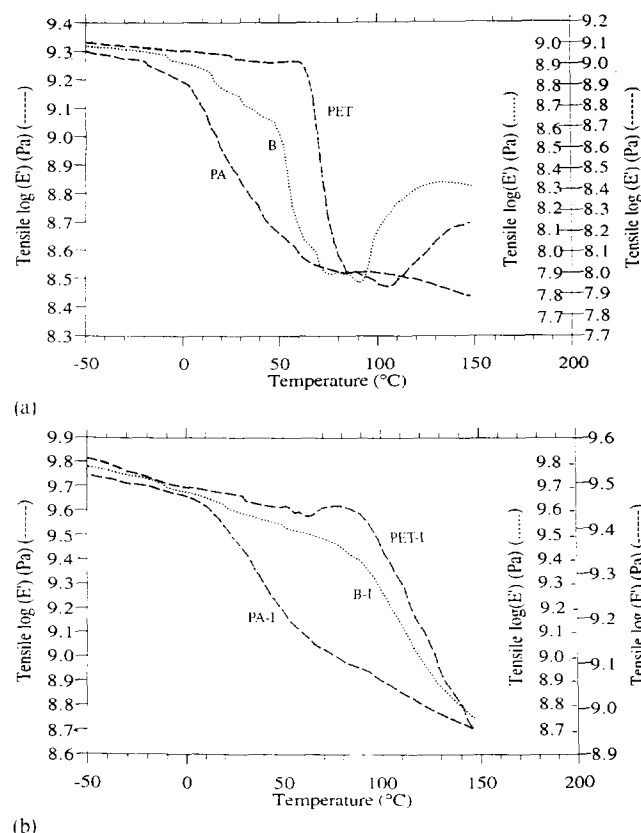


**Figure 2** Temperature dependence of dynamic modulus  $E'$  for neat PET, neat PA and their blend B: (a) as quenched and (b) zone drawn; y-axis scale order (from left to the right): PA, B, PET

1a, the results for an undrawn and unannealed sample (labelled PET) are shown together with those of drawn samples subjected to various thermal treatments (PET-I, PET-I-1, PET-I-2, PET-I-4). The sample designations are given in Table 1. Results for PA samples are displayed in Figure 1b. Likewise, the undrawn, unannealed sample is denoted PA, whereas PA-I, PA-I-1 and PA-I-2 refer to samples subjected to the various thermal treatments.

The maximum in  $E''$  for undrawn and unannealed PET is observed at  $70^\circ\text{C}$ . According to common practice, the maximum of the  $\tan \delta$  curves is considered as the glass transition temperature  $T_g$  ( $\alpha$ -relaxation) of the material. Because a much better resolution is offered by the loss modulus  $E''$  curves,  $T_g$  is evaluated from  $E''$  in the present work. The sample PET-I, which was treated by zone drawing at  $85^\circ\text{C}$ , has the maximum at  $96^\circ\text{C}$ . The peaks of PET-I-1 and PET-I-2, which were subjected to drawing and thermal treatment at increased temperatures prior to DMTA measurements, are both at about  $110^\circ\text{C}$ . The location of the peak for PET-I-4 is shifted to a lower temperature ( $88^\circ\text{C}$ ), compared with those of PET-I-1 and PET-I-2.

In the case of the unannealed, undrawn nylon-6 sample, PA, the maximum in  $E''$  is at  $14^\circ\text{C}$ , as can be observed in Figure 1b. This peak shifts to higher temperatures,  $27^\circ\text{C}$ ,  $23^\circ\text{C}$  and  $32^\circ\text{C}$  for the samples PA-I, PA-I-1 and PA-I-2, respectively, which were drawn and subjected to different thermal treatments as listed in Table 1. In as much as  $T_a = 240^\circ\text{C}$  is above the melting temperature of PA, no further thermal treatment is operative in this case.

The temperature dependences of the storage moduli  $E'$  of PET, PA and their blend B are presented in Figures

2–4. In Figure 2a, results for unannealed and undrawn samples are shown. Results for drawn samples are shown in Figure 2b. Figures 3 and 4 display the storage moduli for drawn samples subjected to different thermal treatments, as indicated by the labels on each curve. It should be noted that for the PA samples, no thermal treatment has been performed at  $T_a = 240^\circ\text{C}$ , this temperature exceeding the melting temperature of PA. Therefore only the results for PA-I-2 are displayed in Figures 4a and b, for comparison with PET and/or PET/PA samples subjected to the higher annealing temperature. In these figures (Figures 2–4), the values on the ordinates refer to PA, blend (B) and PET, respectively in the same order as the curves themselves. The qualitative results are of primary interest in Figures 2–4.

Figure 5 shows the temperature dependences of  $\tan \delta$  (Figure 5a) and loss moduli  $E''$  (Figure 5b) of the PET/PA blends subject to the same mechanical and thermal treatments as their components. The original blend (undrawn, unannealed, sample B) reveals a  $\tan \delta$  curve distinguished by two sharp peaks at about  $70^\circ\text{C}$  and  $100^\circ\text{C}$ , together with a shoulder around  $25^\circ\text{C}$ . A single stronger and broader peak is observed at higher temperatures in all other samples. The shoulder at about  $25^\circ\text{C}$  seems to vanish in B-1, but becomes visible again after thermal treatment in samples B-I-1, B-I-2 and B-I-3, being particularly pronounced in B-I-1. Finally, it disappears in sample B-I-4 which has been subjected to the highest temperature ( $240^\circ\text{C}$ ) annealing for the longest (25 h) duration. A similar behaviour is observed in the  $E''$  data presented in Figure 5b as a function of

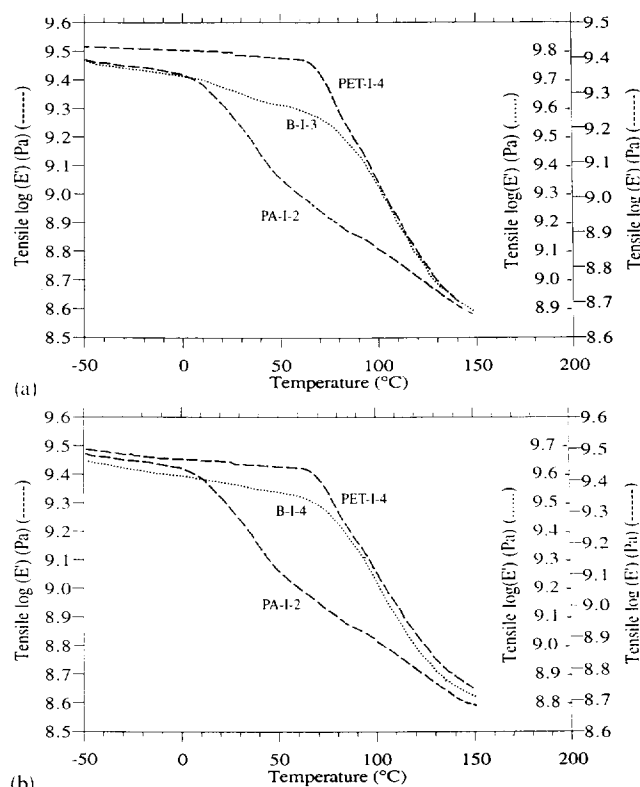


**Figure 4** Temperature dependence of dynamic modulus  $E'$  of zone drawn annealed: neat PA ( $T_a = 220^\circ\text{C}$ ,  $t_a = 25$  h), neat PET ( $T_a = 240^\circ\text{C}$ ,  $t_a = 25$  h) and their blend B annealed at  $T_a = 240^\circ\text{C}$  for: (a)  $t_a = 5$  h and (b)  $t_a = 25$  h; y-axis scale as in Figure 2

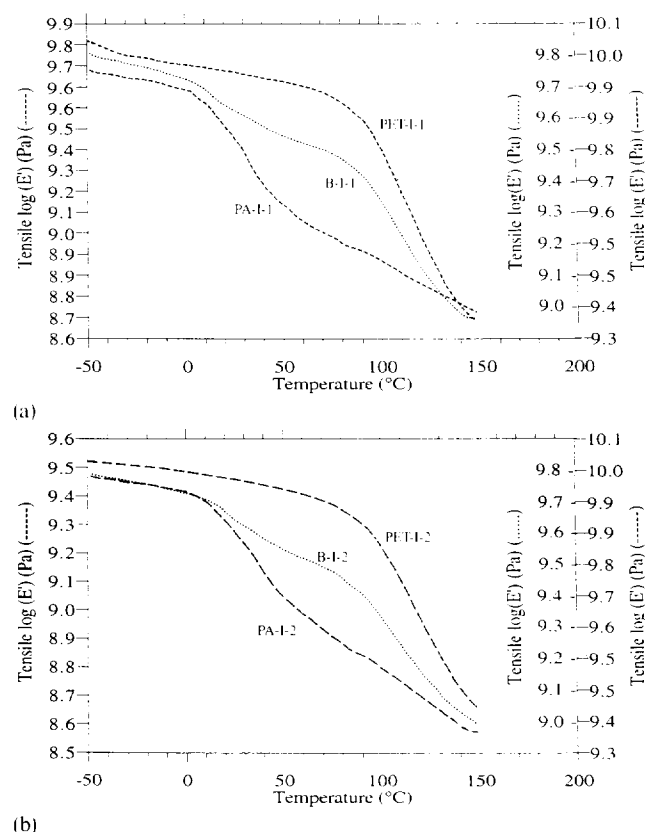


**Figure 3** Temperature dependence of dynamic modulus  $E'$  of zone drawn neat PET, neat PA and their blend B annealed at  $220^\circ\text{C}$ : (a) for 5 h and (b) for 25 h; y-axis scale as in Figure 2

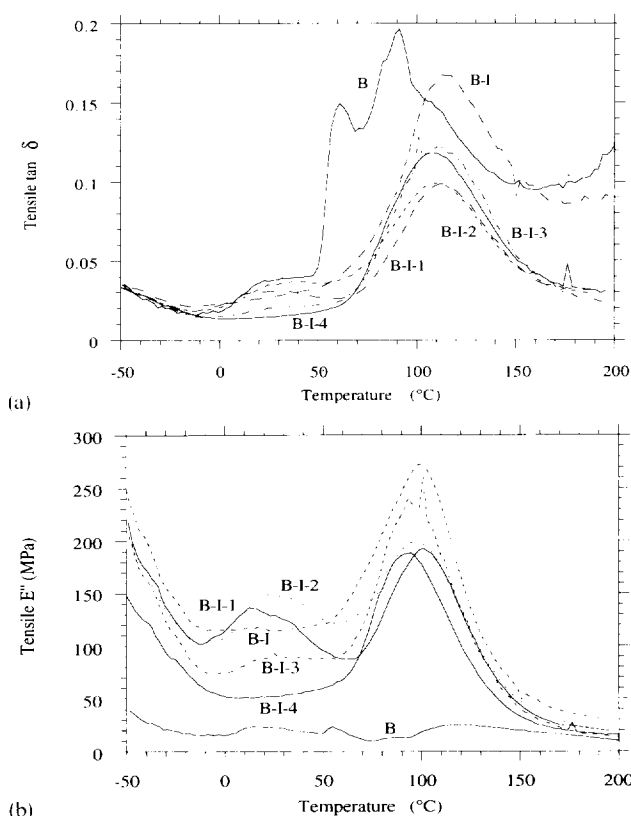


**Figure 5** Temperature dependence of (a)  $\tan \delta$  and (b) loss modulus  $E''$  of blends with different thermal history: B, undrawn, unannealed; B-I, zone drawn; B-I-1, drawn and annealed at  $T_a = 220^\circ\text{C}$ ,  $t_a = 5$  h; B-I-2, drawn and annealed at  $T_a = 220^\circ\text{C}$ ,  $t_a = 25$  h; B-I-3, drawn and annealed at  $T_a = 240^\circ\text{C}$ ,  $t_a = 5$  h; B-I-4, drawn and annealed at  $T_a = 240^\circ\text{C}$ ,  $t_a = 25$  h

temperature. Here, there is a strong peak at about 100°C for all treated samples. The 25°C peak is observed only in the undrawn unannealed blend B, and the thermally treated drawn blends B-I-1, B-I-2 and B-I-3. The sample subjected to zone drawing only (B-I) and that subjected to annealing at  $T_a = 240^\circ\text{C}$  for 25 h do not exhibit that peak, in parallel with the  $\tan \delta$  behaviour displayed in Figure 5a.

## DISCUSSION

In this section, we interpret the various features of the data presented in Figures 1–5. Our interpretation of data is either based on previously established work in this field<sup>5</sup> or suggested as new evidence which has to be tested by future experiments. First, we consider the behaviour of PET and PA in the neat form subjected to various mechanical and/or thermal treatments; then we proceed to the analysis of the behaviour of the blends.

### Glass transition and moduli of neat PET and PA samples

The peak of the PET curve located at 70°C in Figure 1a was attributed in the preceding section to the glass transition of the undrawn, unannealed sample. Similarly, the peaks for PET-I, PET-I-1, PET-I-2 and PET-I-4 appearing at 96, 110, 110 and 88°C, respectively, are identified as the glass transition temperatures. The differences in these  $T_g$  values can be explained by the fact that the glass transition temperature of a semi-crystalline polymer depends strongly on its degree of crystallinity<sup>16–21</sup>. Knowing that PET offers the opportunity to obtain a sample set differing in crystallinity, it has been shown that  $T_g$  for the isotropic amorphous sample first increases (by 50°C), followed by a decrease with continuous rise of the crystallinity<sup>20,21</sup>. The increase in  $T_g$  from 70 to 110°C and also the decrease of  $T_g$  for the sample PET-I-4 can thus be explained. The glass transition temperatures deduced from  $E''$  measurements for different samples are summarized in Table 2.

**Table 2** Glass transition temperatures  $T_g$  of neat PET, neat PA and their blend B (1:1 by weight) subjected to different mechanical and thermal treatments as evaluated by dynamic mechanical thermal analysis

Sample	$T_g$ (°C)			
	$E'$		$E''$	
	$T_g^{\text{PA}}$	$T_g^{\text{PET}}$	$T_g^{\text{PA}}$	$T_g^{\text{PET}}$
PET	–	69	–	70
PET-I	–	100	–	96
PET-I-1	–	103	–	110
PET-I-2	–	108	–	110
PET-I-4	–	78	–	88
PA	12	–	14	–
PA-I	20	–	27	–
PA-I-1	18	–	23	–
PA-I-2	19	–	32	–
B	14	52	23	57
B-I	19	99	–	100
B-I-1	12	101	16	100
B-I-2	19	100	25	98
B-I-3	17	97	25	97
B-I-4	–	80	–	95

In the case of the PA samples, whose loss moduli  $E''$  behaviour is displayed in Figure 1b, all samples exhibit one well resolved single peak, whose location characterizes the glass transition temperature of the samples. However, the inflection point of the curve of storage moduli  $E'$  displayed in Figures 2 and 3 offers another possibility to identify  $T_g$ . The storage moduli curves displayed in Figures 2–4 are distinguished by two relatively flat portions connected by an intermediate region which may be approximated by a straight line. The intermediate region is associated with the softening of the material due to some structural transition, which would be the glass transition in the present case. The inflection point in this intermediate region leads us to the glass transition of the sample. The glass transition temperatures obtained from storage moduli  $E'$  are listed in Table 2. We note that the resulting  $T_g$  values are in good agreement with those deduced from the peaks of the  $E''$  curves.

### Glass transition and moduli of PET/PA blends

The above estimations of the glass transition temperatures of neat PA and PET samples under study will be used in interpreting the  $\tan \delta$  and  $E''$  curves of PET/PA blends displayed in Figures 5a and b. In the case of the untreated blend B, the peak in  $\tan \delta$  at about 70°C is now readily associated with the glass transition of the PET component, whereas the shoulder at around 25°C corresponds to that of the PA component. The highest peak occurring close to 100°C would be assigned to the crystallization of the PET component. An indication of the onset of crystallization is detected both in Figure 2a in which  $E'$  of PET increases from about 100°C and in Figure 1a in which  $E''$  of PET has a relatively weak peak at around 110°C. Likewise in Figure 5b, the three peaks of the loss modulus curve for B would arise from the glass transition of PA, PET and crystallization PET, successively. That the undrawn, unannealed blend exhibits three successive transitions as a function of temperature is also evidenced by the corresponding  $E'$  curve shown in Figure 2a. All these figures (Figures 2a, 5a and 5b) verify the well established fact that untreated PET/PA blends are immiscible. It should be noted, however, that in a previous calorimetric study on the same system only one  $\alpha$ -relaxation peak at  $T_g = 64^\circ\text{C}$  was found<sup>3</sup>. This discrepancy could be explained by the fact that the previous d.s.c. measurements were carried out immediately after the preparation of the film where the present dynamic mechanical study is performed five years later. Phase separation of the two components might have evolved during this period, being particularly enhanced after water absorption and dropping of the glass transition temperature of PA to room temperature. Another reason for the d.s.c. observation can be related to the fact that former measurements were carried out with relatively dry samples and  $T_g$  of PA is supposed to appear much closer to  $T_g$  of PET than in the present case<sup>3</sup>.

Upon zone drawing of the blend, however, some compatibility seems to be induced, as the  $\tan \delta$  and  $E''$  curves for B-I in Figures 5a and b, respectively, suggest. This also conforms with previous detection of only one  $T_g$  by d.s.c. measurements immediately after melt blending<sup>3</sup>. However, the presence of a single apparent glass transition temperature close to that of the neat PET does not necessarily imply the miscibility of the

components at the molecular level. A highly oriented, partially crystalline structure forms at the stage of zone drawing. Zone drawing improves not only the orientation and crystallization but also the dispersity and distribution of the components in the blend so that their compatibility is enhanced. As emphasized by Utracki<sup>5</sup>, in similar cases of immiscible components, the detection of a single concentration-dependent  $T_g$  only signifies that the size of the blend domains is below  $\sim 15$  nm. Utracki further considers the blend behaviour using low-frequency storage modulus as a function of temperature. In the main, a broad and smooth passage between the initial and final flat portions of the  $E'$  curves, as opposed to the sharp decrease observed in neat and/or completely miscible systems, is asserted<sup>5</sup> to be indicative of an immiscible blend with fine dispersion. The latter is also referred to as a compatibilized immiscible blend. The  $E'$ -curve for B-I in Figure 2b exhibits a rather broad transition region conforming with this picture. The fact that the glass transition of the PA component shows up in the drawn samples B-I-1 and B-I-2 subjected to annealing at 220°C lends further support to the argument that the disappearance of the  $T_g$  of PA in B-I should not be readily interpreted as the manifestation of a completely miscible blend. Also, the large  $E''$  and  $E'$  values at 25°C of PET in the drawn blend compared with those in the original untreated blend indicate<sup>18</sup> the decrease in the segmental mobility of the chains or increase in intermolecular friction, which would result from the fine dispersion and dense aggregation of the homopolymers, as previously shown by Kunugi *et al.*<sup>20</sup>.

We now turn our attention to the thermally treated drawn samples, i.e. samples B-I-1, B-I-2 which were annealed at 220°C, and B-I-3 and B-I-4 annealed at 240°C, differing in duration of annealing. The dispersity achieved by zone drawing disappears and separation of the homopolymers takes place by thermal treatment. This is clearly indicated by the appearance of two relaxation peaks in the  $\tan \delta$  and  $E''$  curves for samples B-I-1 and B-I-2, shown in Figures 5a and b, as well as by the shape of the  $E'$  curves of these samples displayed in Figures 3a and b, which is typical of incomplete or limited miscibility in the amorphous regions of the two components. Prolongation of annealing duration at 220°C from 5 h to 25 h has a relatively weak effect on the thermomechanical behaviour of the sample.

Completely different is the behaviour of the samples annealed at 240°C. A strong drop in the intensity of the  $\alpha$ -relaxation peak of the PA component in sample B-I-3 and its complete disappearance after prolonged annealing in sample B-I-4 (Figure 5b) are observed. This suggests some improvement in the miscibility of the components, i.e. some compatibilization induced upon prolonged thermal treatment at high temperature. Two possibilities might be considered for the origin of this apparent improvement in miscibility: first, a fine degree of dispersion, analogous to that of sample B-I, might be achieved again. Second, some chemical, rather than physical, changes might be activated due to treating the sample at sufficiently elevated temperatures.

The shape of the  $E'$  curve of the sample B-I-4 in Figure 4b is very similar to that of sample B-I, and by analogy, the sample B-I-4 could be interpreted as a binary blend with increased degree of dispersion. However, the process of annealing at 220°C resulted in a system exhibiting

distinct biphasic characteristics, as observed from the well resolved peaks for PA and PET components in the  $\tan \delta$  and  $E''$  curves of Figures 5a and b. Thus, treatment at high temperature does not induce any refinement in the dispersion of the two components, but on the contrary, favours their segregation into separate phases. On the other hand, it has been shown that when blends of condensation polymers are treated at relatively high temperatures, close to their melting point, an exchange reaction between the functional groups of the homopolymers is favoured, leading to *in situ* formation of block copolymers<sup>22</sup>. Evidence for such solid-state reactions has been observed in MFCs after annealing at temperatures below but close to the melting temperature of the fibrillized component<sup>1-4,7</sup>. The site for the formation of such copolymers is naturally the interface between the microfibrillar regions and the amorphous matrix. The former is composed predominantly of the PET component whereas molten PA molecules constitute the bulk of the amorphous matrix. Upon prolongation of thermal treatment, layers of block copolymers are shown to grow gradually and at the same time to transform into non-crystallizable random copolymers<sup>7</sup>. Based on theoretical and experimental results concerning copolymers<sup>23-25</sup>, these copolymers should impart some mutual miscibility between the original components. Accordingly, the weakening of the contribution of the PA component to the loss moduli curve in sample B-I-3 and the total disappearance of the PA peak in sample B-I-4 would arise from the fact that the PA component gradually loses its chemical identity through participation in the PET-PA copolymer, and PA homopolymer might eventually be depleted in the sample subjected to a long annealing time. It should be noted that the PET component, on the other hand, maintains its microfibrillar structure to a large extent, only the parts of it in the amorphous regions of microfibrils being involved in copolymerization reactions.

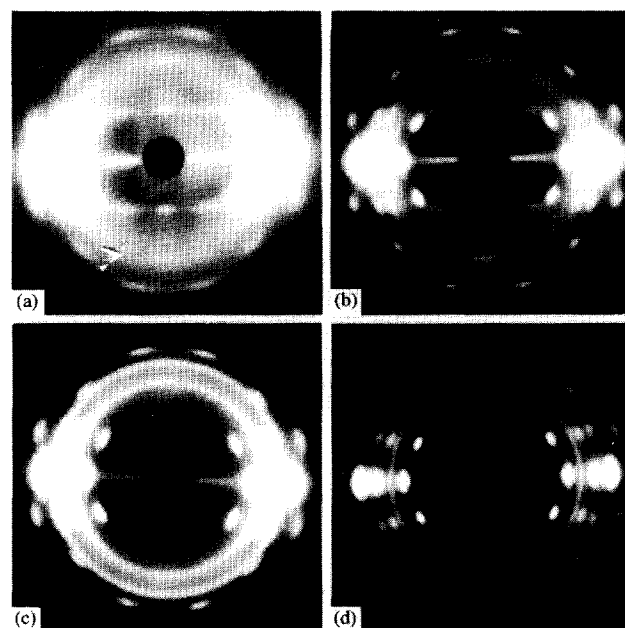


Figure 6 WAXS patterns taken after different stages of the treatment of PET/PA blend (1:1 by weight): (a) B-I, (b) B-I-1, (c) B-I-3, (d) B-I-4

For a further assessment of the mechanism responsible for the apparent compatibility of the components in the sample B-I-4, WAXS patterns taken at the same stages of preparation of MFC have been considered. These are displayed in *Figure 6*. One can see in *Figure 6a* that drawing results in the orientation of both components in the blend while annealing at 220°C leads to considerable improvement of orientation and crystalline structure (*Figure 6b*). Drastic changes in the blend happen after annealing at 240°C. PA melts during annealing, and after subsequent cooling it crystallizes again but is no longer in an oriented state. At this stage (*Figure 6c*) a MFC is produced. Upon prolongation of annealing to 25 h at 240°C and cooling again, PA disappears as an independent crystalline phase (*Figure 6d*). This elevated annealing temperature, just below the melting temperature of PET, favours the transreactions between the amorphous part of PET and the molten PA. The transreaction apparently proceeds until the entire amount of PA, which is in the molten state at this temperature, participates in a random, non-crystallizable copolymer. The disappearance of the  $E''$  peak in the sample B-I-4 would likewise be interpreted as the exhaustion of the PA homopolymer in the amorphous regions, the latter being used up in the formation of the copolymer.

## CONCLUSIONS

The following conclusions are drawn from the present study:

1. Dynamic mechanical thermal measurements offer a practical means for establishing the miscibility and compatibility of the homopolymers in MFC through examination of the amorphous phases. Nevertheless, simultaneous consideration of the  $\tan \delta$ , loss and storage moduli curves is important for a correct interpretation of the measurements although the maximum of  $\tan \delta$  is systematically increased (by about 6 or 8°C) as compared with the maximum of  $E''$  and to the inflection point of  $E'$ . Determination of  $T_g$  from the temperature dependence of  $E'$  and  $E''$  as opposed to  $\tan \delta$  curves seems to be more precise and reliable.
2. Drawing of the sample is observed to induce some compatibilization, although at the molecular level the PET and PA components preserve their immiscibility, since distinct phases emerge upon annealing of the samples. Thus, annealing at 220°C enhances the reorganization of the homopolymers within distinct phases and thus reveals the inherent immiscible character of the components.
3. The possibility of the occurrence of chemical reactions leading to copolymers at phase boundaries should not be overlooked if the annealing is performed at a sufficiently high temperature for a long duration. Here, annealing at 240°C appears to have activated transreactions between the molten PA and the PET molecules located in the amorphous parts of the microfibrils. Such reactions may result in MFCs with substantially different thermomechanical characteristics, in as much as the low melting component (PA) may be completely involved in a random copolymer formation and consequently lose its amorphous and crystalline phase characteristics.
4. In conclusion, this dynamic mechanical study on PET/PA blend draws attention, in agreement with previous work, to the fact that blends of condensation polymers offer additional opportunities for overcoming their incompatibility, owing to their inherent ability to undergo chemical interactions at phase boundaries during processing.

## ACKNOWLEDGEMENTS

The financial support from Bogazici University Research Fund No. 94P0002 is gratefully acknowledged as well as the partial support of the Ministry of Science and Education, Bulgaria and of the NSF, USA, Grant no. INT-9307812.

## REFERENCES

1. Evstatiev, M. and Fakirov, S. *Polymer* 1992, **33**, 877
2. Fakirov, S. and Evstatiev, M. 'The Interfacial Interactions in Polymeric Composites' (Ed. G. Akovali), Kluwer Academic, Dordrecht, 1993, p. 417
3. Fakirov, S. Evstatiev, M. and Schultz, J. M. *Polymer* 1993, **34**, 4669
4. Fakirov, S., Evstatiev, M. and Petrovich, S. *Macromolecules* 1993, **26**, 5219
5. Utracki, L. A. 'Polymer Alloys and Blends. Thermodynamics and Rheology', Hanser, Munich, 1989
6. Kimura, M. and Porter, R. S. *J. Polym. Sci., Polym. Phys. Edn* 1983, **21**, 367
7. Fakirov, S. 'Solid State Behavior of Linear Polyesters and Polyamides' (eds J. Schultz and S. Fakirov), Prentice Hall, Englewood Cliffs, NJ, 1990
8. Devaux, J., Godard, P., Mercier, J. P., Touillaux, R. and Derepec, J. M. *J. Polym. Sci., Polym. Phys. Edn* 1982, **20**, 1881
9. Devaux, J., Godard, P. and Mercier, J. P. *J. Polym. Sci., Polym. Phys. Edn* 1982, **20**, 1901
10. Devaux, J., Godard, P. and Mercier, J. P. *J. Polym. Sci., Polym. Phys. Edn* 1982, **20**, 1895
11. Devaux, J., Godard, P. and Mercier, J. P. *J. Polym. Sci., Polym. Phys. Edn* 1982, **20**, 1875
12. Kimura, M. and Porter, R. S. *J. Polym. Sci., Polym. Phys. Edn* 1983, **21**, 367
13. Miley, D. M. and Runt, J. *Polymer* 1992, **33**, 4643
14. Kunugi, T., Suzuki, A. and Hashimoto, M. *J. Appl. Polym. Sci.* 1981, **26**, 1951
15. Kunugi, T., Akiyama, I. and Hashimoto, M. *Polymer* 1982, **23**, 1193
16. Illers, K. H. *Makromol. Chem.* 1968, **38**, 168
17. Bell, J. P. and Murayama, T. *J. Polym. Sci. (A-2)* 1969, **7**, 1059
18. Dumbleton, J. M. and Hashimoto, M. *Kolloid. Z. Z. Polym.* 1967, **220**, 431
19. Simov, D., Fakirov, S., Michailov, M. and Petrenko, P. *Vysokomol. Soed.* 1973, **15A**, 1775
20. Kunugi, T., Ikuta, T. and Hashimoto, M. *Polymer* 1982, **23**, 1983
21. Simov, S., Fakirov, S. and Mikhailov, M. *Kolloid. Z. Z. Polym.* 1970, **238**, 521
22. Flory, P. J. 'Principles of Polymer Chemistry', Cornell University Press, Ithaca, NY, 1953
23. Allport, D. C. and Mohaier, A. A. 'Block Copolymer' (eds D. C. Allport and W. H. Janes), Wiley, New York, 1973
24. Meier, D. J. *J. Polym. Sci. (C)* 1969, **26**, 81
25. Robeson, I. M., Matzner, M., Fetters, I. J. and McGrath, J. E. 'Recent Advances in Polymer Blends, Grafts, and Blocks' (Ed. I. H. Sperling), Plenum, New York, 1974